2007

CHARACTERIZATION OF LONG PATHLENGTH CAPILLARY WAVEGUIDES FOR EVANESCENT FLUORESCENCE APPLICATIONS

Eric Paprocki
The University of Montana

CHARACTERIZATION OF LONG PATHLENGTH CAPILLARY WAVEGUIDES FOR EVANESCENT FLUORESCENCE CHARACTERIZATION

By

Eric Daniel Paprocki

B. S., Chemistry, State University of New York College at Fredonia, Fredonia, NY, 2002

Thesis

presented in partial fulfillment of the requirements
for the degree of

Master of Science
in Chemistry

The University of Montana
Missoula, MT

Summer 2007

Approved by:

Dr. David A. Strobel, Dean
Graduate School

Dr. Michael DeGrandpre, Chair
Chemistry

Dr. Christopher Palmer
Chemistry

Dr. William Laws
Chemistry

Dr. Michele McGuirl
Biology

Paprocki, Eric, M.S., Summer 2007 Chemistry

Characterization of long pathlength capillary waveguides for evanescent fluorescence sensing applications

Chairperson: Michael DeGrandpre

The optical properties of a novel fused silica fiber-optic capillary waveguide (FOCap) for fluorescence spectroscopy were evaluated. Evanescent fluorescence from samples in the FOCap was measured by coupling the FOCap to a light source and a fluorescence spectrophotometer. The FOCap has negligible excitation light loss over long lengths (20 m or more) for a range of wavelengths. The evanescent fluorescence was linear up to at least 20 m for a solution in the core and up to at least 15 m for a fluorophore covalently attached to the inner surface. Evanescent fluorescence measurements in 50, 150, and 250 μm inner diameter FOCaps indicate that greater sensitivity is achieved with thinner-walled capillaries which have more internal reflections. FOCaps can be fined tuned for a desired sensitivity by manipulating their physical dimensions. The ability of the FOCap to function as an indirect chemical sensor for nitroaromatic compounds is demonstrated with a pyrene-labeled waveguide.

ACKNOWLEDGEMENTS

I would like to thank Michael DeGrandpre for his support and guidance throughout this project and Bill Laws for his expertise in the early stages and beyond. Special thanks go to Ruben Darlington for design and production of several of the components used in experiments. I would also like to thank my coworkers in the DeGrandpre and Ross labs for their input and support as well as my other committee members, Chris Palmer and Michele McGuirl.

This research was sponsored by the Army Research Laboratory and was accomplished under Cooperative Agreement Number W911NF-04-2-0043.

Of course, I would like to thank my parents, Stephen and Sue Paprocki and my friends and other family for all their encouragement and support.

TABLE OF CONTENTS

LIST OF TABLES

LIST OF FIGURES

Chapter 1

Introduction

A number of optical fluorescence sensors have taken advantage of the surface selectivity of the evanescent wave (EW). Sensor configurations that utilize evanescent wave fluorescent spectroscopy (EWFS) include resonant mirrors, interferometers, surface plasmon resonance sensors, fiber optic, and planar arrays [1]. Fiber optic fluorescence sensors have found, in recent years, increasing use for monitoring of environmental conditions (pH, temperature, pressure, radiation) and for detection of chemical or biological analytes (pollutants, toxins, antibodies, explosives, chemical weapons, etc.) [2-5]. In most of these sensors, fluorescence is excited just outside the boundary of a waveguide through interaction with the EW associated with the trapped modes guided under the principle of total internal reflection (TIR). A trapped mode has a field intensity that decays monotonically in the transverse direction everywhere external to the core and does not lose power to transmitted radiation. The fluorescence emission available for detection is that which is captured by the trapped modes of the waveguide.

The sensitivity limits of EWFS depend on the number of total internal reflections, the depth of penetration of the evanescent field at each reflection interface, and the fluorescence collection efficiency [6]. Low depth of penetration limits the fluorescence sensitivity of short length waveguide transducers with low total reflections [7].

Fluorescence methods hold inherent sensitivity advantages over absorption techniques. EWFS has improved selectivity over analogous absorption methods that suffer from non-specific absorption of sample components and often require additional

pretreatment steps. Background fluorescence from other compounds in a sample matrix can greatly hinder a chemical sensor so fluorophores chosen for a particular detection scheme should be selected while keeping this in mind.

Generally, in evanescent wave fiber optic sensors (EWFOS), a chemical species (e.g. a fluorophore) is probed in the cladding layer of the waveguiding structure or in a cladding-stripped area of the fiber [7]. Detection limits are poor for sensors that rely on probing interactions at stripped fiber optic interfaces because fragility of bare fibers limits the transducer length [6]. More recently, waveguiding capillaries have been employed to improve sensitivity and environmental exposure problems inherent in many EWFOS [8-13]. Capillary waveguides can alo function as both optical and sampling cells in evanescent wave (EW) based chemical sensors.

A Couple of examples of EW capillary fluorescence sensors have been reported in the literature. Kessler, *et al* demonstrated a capillary waveguide fluorescence sensor for human serum albumin in urine. They achieved a detection limit of 1 mg/L in a short capillary waveguide[14]. A nucleic acid sensor capillary waveguide has been developed along with design guidelines for optimizing the collection of free propagating fluorescence for capillary waveguide sensors[10]. A sensitivity of 30 pg/mL was achieved in a 10 cm segment. The response time of both of these sensors was very fast and only limited by sample pumping.

Doped fused silica micro-capillary waveguides have recently become commercially available. This fiber optic capillary (FOCap) consists of a fused silica wall which serves as the light guiding region, surrounded by the doped silica cladding and a polyimide coating (Fig. 1). Like conventional fused silica optical fibers, FOCaps can guide light in

the wavelength region from the UV to the near infrared. The surrounding polyimide coating layer makes the tubing flexible and thereby able to be bent in a tight radius so, unlike conventional fibers, long pathlength, compact EW fluorescence sensors can potentially be achieved with FOCaps.

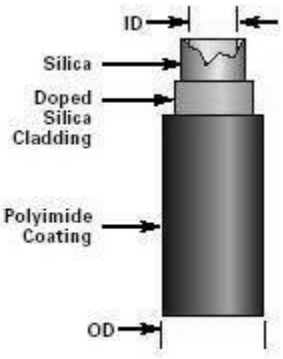

Fig. 1. Schematic of the commercially available fiber optic capillary (FOCap) (picture courtesy of Polymicro Technologies, LLC).

In addition to long pathlength sampling, FOCaps also hold advantages over conventional fiber optic sensing elements due to small sample volume requirements and the ability to probe selective reactions at a protected interface. For selective optical sensing, probe molecules can be covalently bound to the interior surface of the capillary to provide detection of target molecules flowing through the capillary [15,16]. Having the reagent coating on the inner portion of the waveguide structure allows for easier handling and protection from environmental damage as compared to conventional fiber optic sensors. Also, like conventional fiber optics, FOCaps can serve as wavelength discriminating elements, having excitation light and emission light traveling in opposite directions.

A few recent studies have used the FOCap for evanescent absorbance spectroscopy applications [15-17]. Keller *et al.* investigated various parameters that control evanescent

absorbance sensitivity for FOCap designs [15,17]. Evanescent absorbance response dependence on the physical dimensions of the FOCap (ID and length) and analyte concentration for a bulk solution held in the capillary were tested. The liquid core waveguiding (LCW) properties of FOCaps were also examined and the FOCap was found to have a shorter effective pathlength than conventional polyimide-coated glass capillaries when used as LCWs.

A few reagent-based FOCap sensors have been developed [15-18]. Tao *et al.* used FOCaps to develop three absorbance sensors for Cu(II), toluene in water samples and ammonia in gas samples[16].

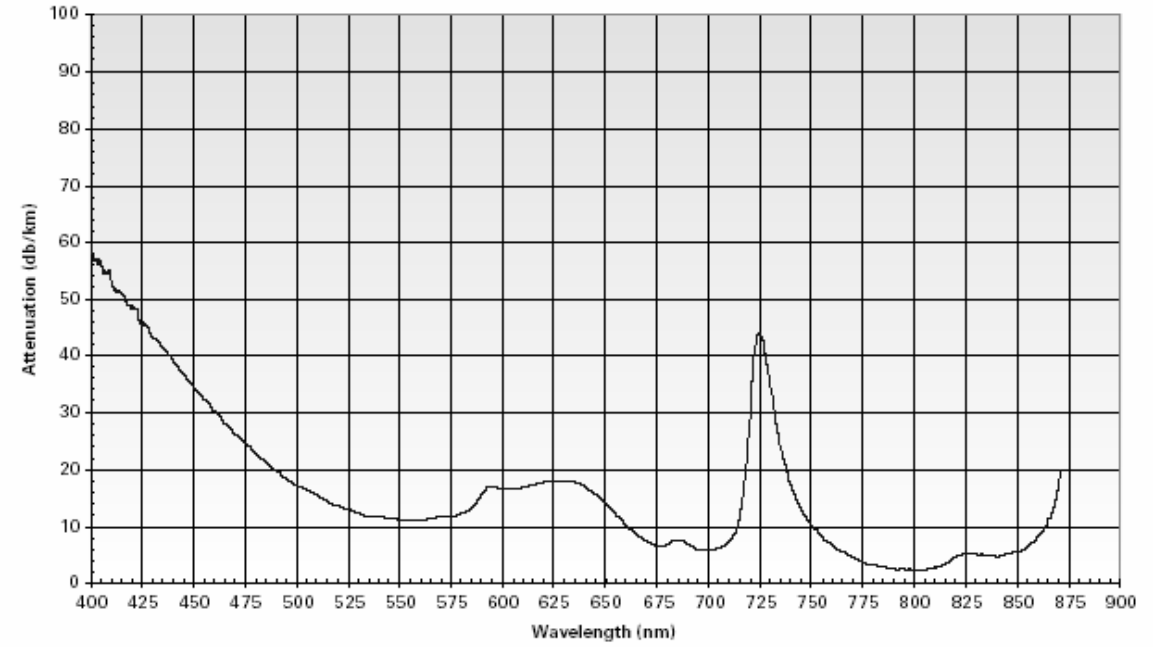

Fig. 2. Optical transmission preliminary data from 150 μm ID FOCap. Standard cut-back attenuation on 253 m segment as reported by Polymicro Technologies, LLC (picture courtesy of Polymicro Technologies, LLC).

In order to develop effective FOCap-based fluorescence sensors, it is imperative to understand their evanescently excited fluorescence guiding properties. The initial goal of our studies was to confirm the reported optical attenuation properties (Fig. 2) of the novel

product (FOCap, LTSP series, Polymicro Technologies, LLC) while devising a system for exciting fluorescence and collecting emission from capillary waveguides and allowing the simultaneous flow of fluid through the capillary bore hole. For the bulk of this M.S. research, the aim was to determine the evanescent fluorescence sensing properties of the FOCap. Evanescent fluorescence is tested for a fluorophore solution, 3,3'-Diethylthiacarbocyanine Iodide (DTCC) (Fig. 3) held in the core with varying concentrations and FOCap physical dimensions. DTCC was used in these studies because it could be excited with an available laser and because it also proved useful in absorbance studies. Evanescent fluorescence is tested against FOCap ID and length. Evanescent

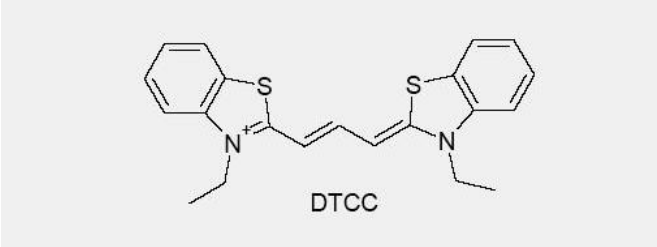

Fig. 3. Structure for 3,3'-Diethylthiacarbocyanine Iodide.

fluorescence is also tested with two different fluorophores covalently attached to the inner fused silica waveguiding structure.

In initial proof of concept studies, the fluorophore fluorescein is covalently attached to the inner wall to develop a uniform labeling procedure. Later, in separate experiments, the fluorophore pyrene is immobilized to examine the fundamental sensing properties of FOCaps and to also determine FOCaps' usefulness as optical chemical sensors. In this application, nitrated compounds are detected indirectly via the quenching of pyrene.

Pyrene is effectively and, to a degree, selectively dynamically quenched by nitroaromatics and nitroaliphatics [19].

Nitroaromatic and nitramine explosives are common and important components of energetic compounds. Reliable identification of explosive compounds in preblast air samples and postblast residues is of great importance to security personnel. In addition, contamination of ground and surface waters with energetic compounds in and around military installations is of concern. Currently employed detection systems do not achieve adequate sensitivity and selectivity [20-23].

Selective fluorescence quenching can be used to analytical advantage in identifying explosive compounds when applied in a carefully controlled way. When a fluorophore is

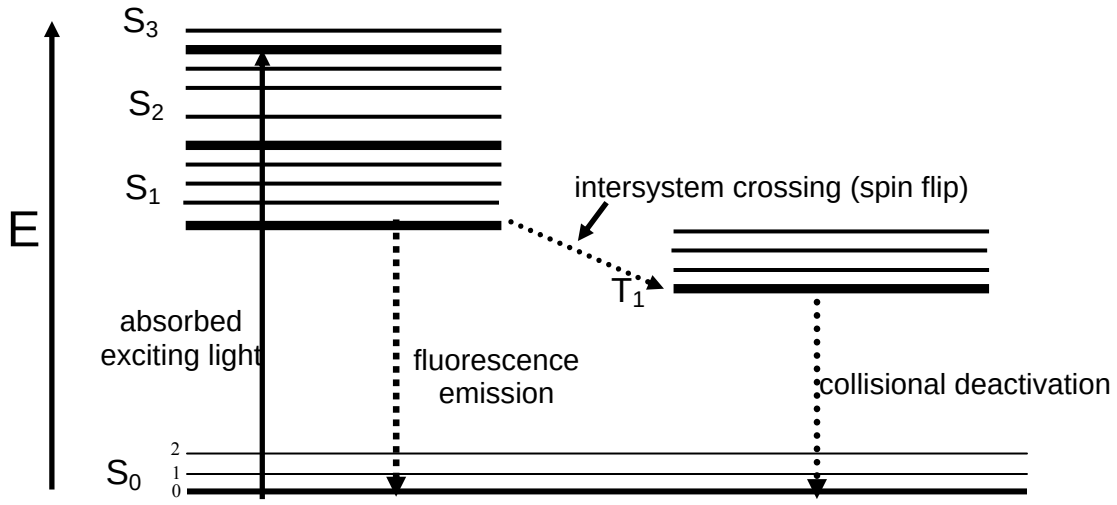

Fig. 4. Jablonski diagram. Dynamic fluorescence quenching causes a spin flip and intersystem crossing and collisional deactivation of the fluorophore.

excited to a S_1 , S_2 ,or S_3 state it normally, in the absence of quencher, loses energy through vibrational relaxation or internal conversion, to the lowest excited S state, where it then returns to a vibrational level of the ground state S_0 via fluorescence i.e. emission

of a photon (Fig. 4). In dynamic quenching, intersystem crossing occurs whereby a quenching molecule causes a spin flip in the excited fluorophore and the fluorophore shifts to a lower energy triplet state. Energy is then lost through radiative or non radiative decay (no fluorescence).

When a pyrene analogue is covalently bound to the surface of a FOCap, liquid solutions or gas phase samples with a suspected presence of nitrated compounds can be pumped through the capillary and a concentration-dependent decline in fluorescence monitored. In this study, 2,4-dinitrotoluene (2,4-DNT) is used as a representative compound for trinitrotoluene (TNT) as it is a common by-product of TNT production as well a TNT breakdown product.

The theory for the origin of the signal in capillary EWFS as well as basic theory for fluorescence quenching are presented in this thesis. The multiple experimental setups used and sample preparation and labeling procedures will be described in detail. Background fluorescence and the steps taken to eliminate its contribution to overall measurements are discussed. Results and discussion focus on important results found in light throughput, fluorescein labeling, pyrene labeling and fluorophore solution in core experiments.

Chapter 2

Theory

2.1 Evanescent fluorescence in FOCaps

The principle of total internal reflection (TIR) states that light launched into a waveguide with refractive index n_1 will reflect all the light within the waveguide when the angle of incidence of light propagating within the waveguide, θ, is greater than the critical angle, θ_c, (Fig. 5, point B) as defined by:

$$\theta_c = \sin^{-1}\left(\frac{n_2}{n_1}\right), \qquad (2)$$

where n_2 is the surrounding media of next lower refractive index.

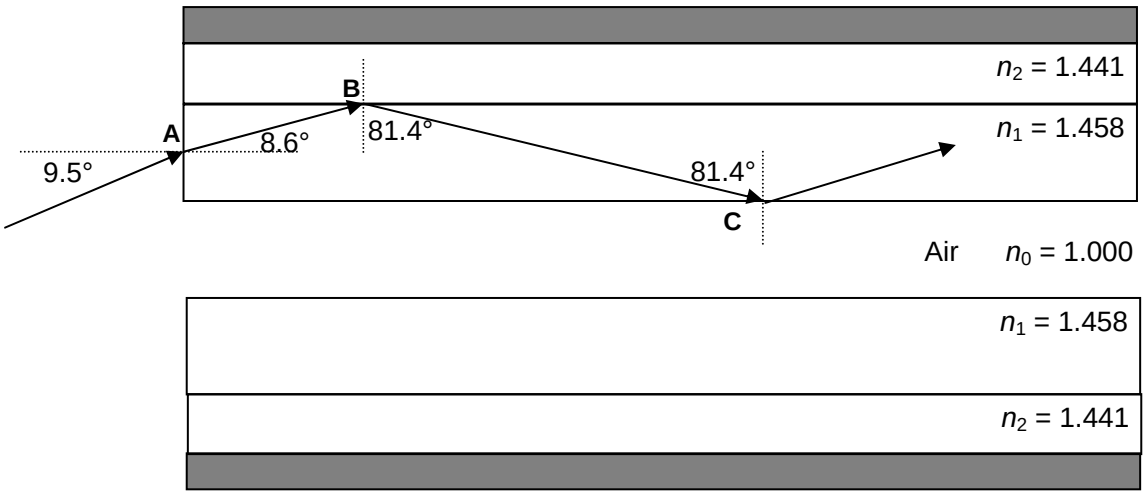

Fig. 5. Ray-tracing diagram of a FOCap for light entering the waveguide at its end face. Refractive indices are labeled on the right and correspond to the doped fused silica cladding (n_2 = 1.441), synthetic fused silica capillary wall (n_1 = 1.458), and the capillary core (air filled, n_0 = 1.000). In a numerical aperture matched system, light approaches the capillary end face relative to the longitudinal normal at 9.5° or less and is refracted into the glass at point A. The light is totally internally reflected at point B (81.4° > 81.2° (Θ_c)) and again at point C (81.4° > 65.7° (Θ_c)) (see Theory). The shaded region is the protective polyimide coating. The layers are not drawn to scale. Wall thicknesses ranges from ~40 μm (250 μm ID) to ~140 μm (250 μm ID).

Under TIR conditions, the Fresnel transmission coefficients (measure of how much light passes through a surface or an optical element) for the transverse electric wave and the transverse magnetic wave are non-zero [24]. So, although light energy is totally reflected, an electromagnetic field extends out from the surface into the lower index medium. This field is the evanescent wave and it decays exponentially with distance from the surface, and is generally effective out away from the waveguide surface to a distance of approximately 100 nm to the wavelength of the incident light. The distance from the surface at which this strength is 1/*e* of its value at the surface is known as the depth of penetration (d_p) and is a function of the refractive indices, the angle of incidence, and wavelength:

$$d_P = \frac{\lambda}{2\pi(n_1^2 \sin^2\theta - n_2^2)^{1/2}} \tag{3}$$

where n_1 corresponds to the light guiding section and n_2 is the refractive index of the doped layer of the waveguide (n = 1.441) or the capillary core. The depth of penetration increases with longer wavelengths and increasing launch angles (θ), with a maximum at θ_c (relative to a normal perpendicular to the fiber axis as shown in figure 5). Propagating light is attenuated as its evanescent field interacts with absorbing species near the interface. Due to the exponential decay of this field strength, transducible optical signals are limited to within a certain distance from the waveguide's surface and as such optical interferences from components in the lower index medium are thus minimized. In the FOCap, the critical angle is set by either the doped layer or core, whichever has the higher refractive index below that of fused silica. For an aqueous solution, the outer wall with n = 1.441 will set the range of propagating angles; however, the aqueous solution (n = 1.33) controls the depth of penetration in Equation 3 into the sensing region for a given

propagating angle. If the core refractive index is larger than 1.441, the FOCap has both wall-guided and core-wall guided modes and behaves, in part, as a liquid core waveguide[12].

In EWFS, the signal level is proportional to the evanescent absorption and to the fraction of emitted fluorescence reaching the detector. The general expression for the signal from an evanescent wave fluorescence sensor can be written as:

$$S_{EWFS} = kA_e E_c \,, \tag{4}$$

where S is the signal, A_e is the evanescent absorption, E_c is the fraction of emitted fluorescence reaching the detector (collection efficiency), and k is a proportionality constant incorporating fluorescent quantum efficiency, evanescent excitation intensity, and the spectral transmission of the optics and detector response. E_c and A_e are maximized when the sensor's numerical aperture (NA) and optical system's NA are matched[25]. To find the total efficiency of light collected from a sample in EWFS, the principal of reciprocity must be invoked[26]. The principal states that the angular dependence of fluorescence tunneling back into a waveguide from a sample is proportional to the angular dependence of the original evanescent field intensity exciting the sample. The magnitude of A_e and E_c depend only on the intensity of the evanescent field as expressed by the Fresnel transmission coefficient at waveguide boundary-sample interface. The relationship for evanescent absorption in FOCaps is [17]:

$$A_e \propto \frac{\alpha L \lambda}{\rho NA}, \tag{5}$$

where λ is the wavelength, L is the length of the capillary, ρ is capillary wall thickness and α is the bulk absorption coefficient ($\alpha = \varepsilon c$). Because quantum efficiency, collection

efficiency, *NA*, and spectral transmission of the optics remain constant for the measurements performed and reported here, they are combined to form the constant *k* in the final expression for EWFS in the FOCap:

$$S_{EWFS} = k\frac{\alpha L \lambda}{\rho} \quad . \tag{6}$$

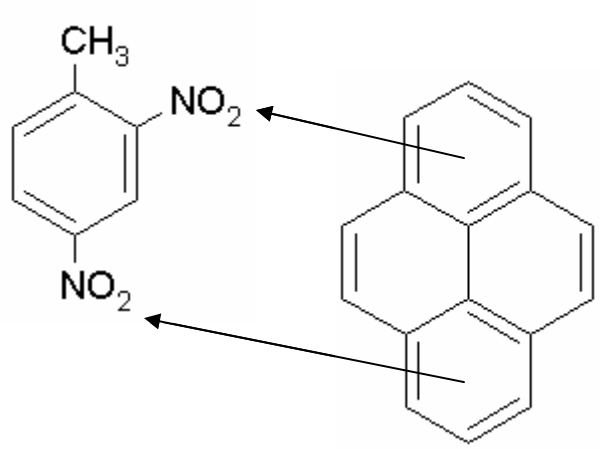

Fig. 6. A charge transfer complex is formed between an excited state pyrene molecule and a ground state quencher, 2,4-DNT. The strong electron withdrawing ability of nitrated compounds allows them to form strong charge transfer complexes with fluorophores such as polycyclic aromatic hydrocarbons.

2.2 Dynamic Quenching

The Stern-Volmer equation describes the dynamic quenching interaction: [27]

$$\frac{F_0}{F} = 1 + k_q \tau_0 [Q] = 1 + K_D [Q], \quad (7)$$

where F_0 and F are the fluorescence counts in the absence and presence of quencher, respectively, k_q is the bimolecular quenching constant, τ_0 is the unquenched lifetime of the fluorophore, *[Q]* is the quencher concentration, and K_D is the linear Stern-Volmer quenching constant.

Oxygen is present in non-aerated solutions at a concentration of ~1 x 10^{-3} M and normally reduces the fluorescence of a typical compound by around 20%. The ratio of observed fluorescence in aerated and non-aerated solution is given by L_0/L. For pyrene this value is 1.0, so oxygen has little or no effect on its luminescence [28]. If pyrene is present in high enough concentrations, an excimer can form that is more sensitive to oxygen quenching.

Chapter 3

Methods

3.1 Experimental Apparatus

As with most fluorescence-based analyses, the detection limit (DL) in EWFS is largely determined by the amount of photons emitted by the fluorophore, the amount of these photons collected by the optics and the extent of stray excitation light bleeding into the emission band. To achieve low DLs, optimal design based on a combination of optical filtering, high-speed optics, and a sufficient separation of the excitation and emission bands is essential [10]. Various optical configurations have been used in previous capillary and fiber waveguide-based fluorescence sensors [9,10,29,30] (Fig. 7). A coaxial arrangement is commonly used where excitation and emission light travel, and are filtered out and collected, respectively, as they exit the capillary and/or fiber. This configuration requires substantial optical filtering to remove the excitation light.

As stated above, closely matching the optical system's numerical aperture (NA) to the sensor's NA is also critical to achieving a strong signal for fiber-based EWFS [24]. Nearly all the power present in an evanescent wave comes from the higher order modes, which are those with the largest propagation angles with respect to the normal to the fiber axis, shown in Fig. 5 at points B and C. The higher order modes are best filled when launching at the sensor's NA. By matching the waveguide NA, insures that light will propagate over the full range of acceptance angles.

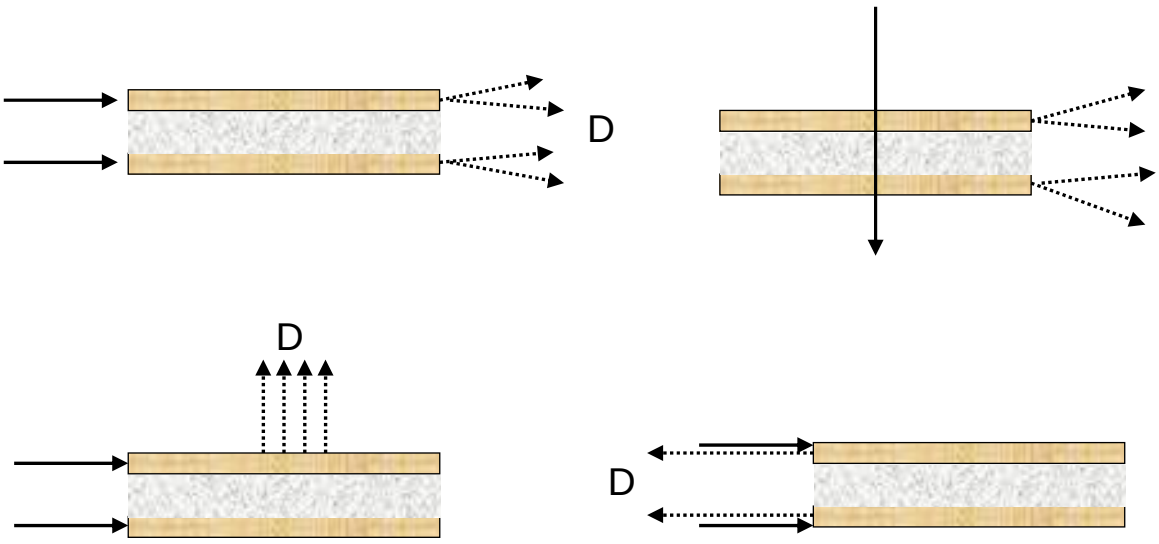

Fig. 7. Various optical configurations used in EWFS in previous capillary waveguide studies. Solid lines represent excitation light and dashed lined emission. D is to the detector.

In this work, light was launched through either an objective illuminating the end face of an index matched fiber (bulk fluorophore solution case, fluorescein labeled capillaries) or with a commercial fiber optic coupler (covalently attached fluorophore case). No attempt was made to alter light launch angle in either case. When designing each experimental apparatus, achieving high light throughput was essential. Light throughput measurements were taken and throughput optimized through positioning and polishing of optical materials. All ends of capillary and fiber were mechanically polished for increased light throughput prior to insertion in experimental apparatuses. Periodic checks on throughput were performed between measurement sets at the distal region(s) of the setups. Re-polishing and/or repositioning of materials were performed as needed. Spectra were corrected to constant light throughput relative to an average of power meter

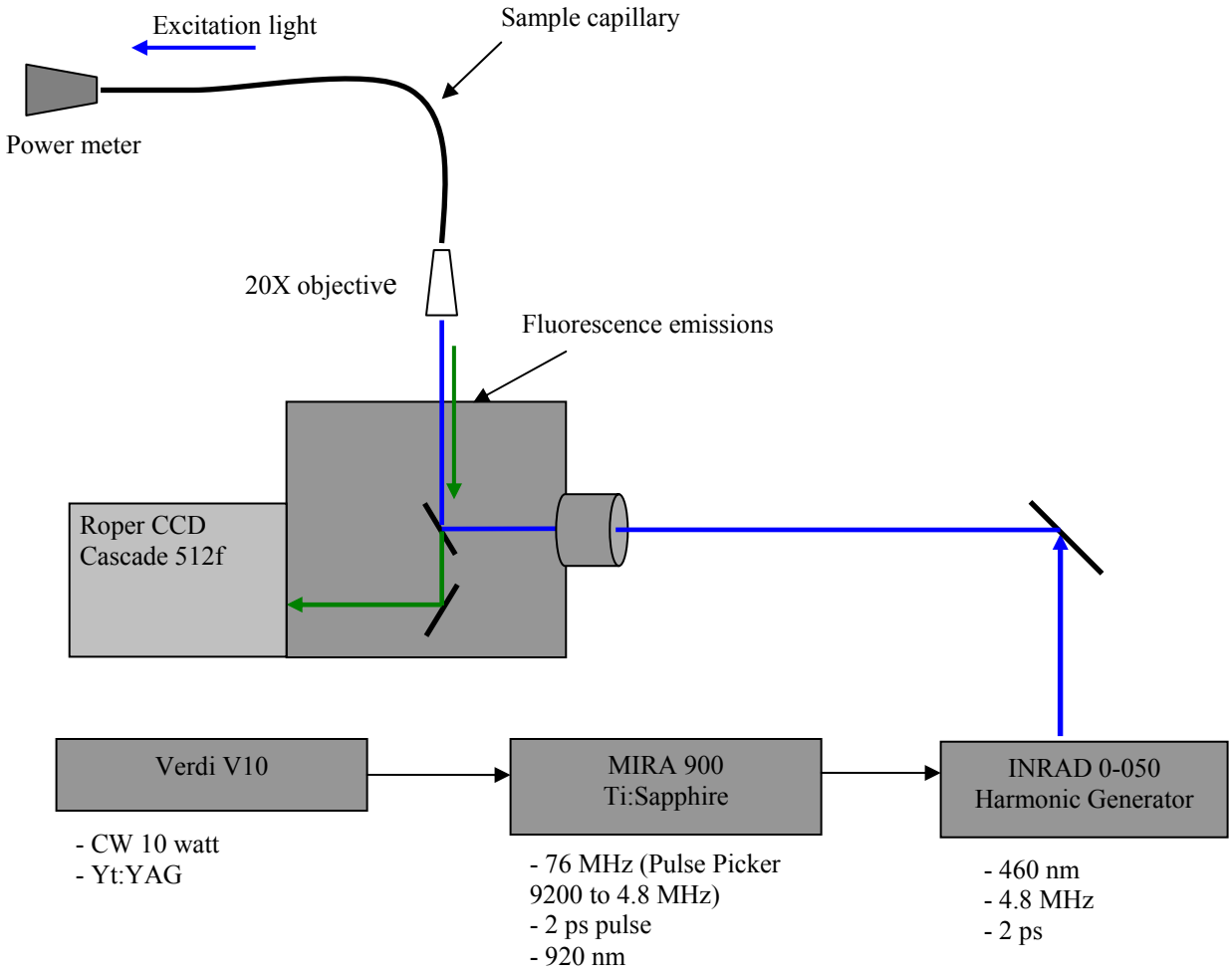

Fig. 8. Apparatus used in FITC-labeled FOCap experiments.

reading. The average power meter reading at the distal end of each setup was 1.94 μW for FITC excitation, 0.54 μW for DTCC, and 1.52 for pyrene.

For early light throughput and fluorescein experiments, the University of Montana's BioSpectroscopy Core Facility was utilized. The experimental setup for fluorescein measurements is diagramed in Fig. 8. For the light source, a Ti:Sapphire laser (Coherent Mira900 ps/fs, tunable IR, 76 MHz (Pulse Picker 9200 to 4.8 MHz, 2 ps pulse, 920 nm) is

pumped by Yt:YAG laser (Verdi V10, CW, 10 W). The 920 nm output light of Ti:Sapphire laser is frequency doubled with a harmonic generator (INRAD 0-050, 4.8 MHz, 2 ps) to give 460 nm laser light. Light is directed into an inverted fluorescence microscope (Axiovert) where it passes through a notch filter (HQ470/40X, Chroma Technology Corporation), reflects off a dichroic mirror (HQ525/50M, Chroma Technology Corporation), before passing through a 20x microscope objective and then to the capillary. Evanescent fluorescence emissions from the capillary traveling in the opposite direction as excitation light are collected by the objective, pass through the dichroic mirror and long pass filter (HQ500LP, Chroma Technology Corporation) before being detected by a CCD camera (Roper Cascade 512f). A power meter (LaserMate-Q, Coherent, Inc.) is placed at the distal end of the capillary to monitor fluctuations in light intensity from the laser. Background fluorescence emissions from the polyimide coating proved particularly problematic for this experimental setup and with the labeling procedure used early on. Therefore 0.5 cm of the polyimide was removed from the capillary end faces with a torch. Images of the capillary end faces taken by the CCD camera for the 50 μm and 150 μm ID FOCaps appear in Fig. 9. Inconsistencies in coloring on the end faces is due to non-uniformities in the polished surface and also because coherent (laser) light destructively interferes in a waveguide.

To determine the light throughput capabilities of FOCaps, a pinhole is placed in the path of the laser light (460 nm) and a measurement is recorded from the power meter at that point. A lens (NT46-266, Edmund Optics F/# 2.27) focuses light onto the end face of a FOCap held in place by a fiber chuck in an x-y-z positioner. The distal end of the

FOCap is held in place by another fiber chuck/positioner and held to the sensing surface of the power meter. The FOCap is then positioned at the proximal end to the highest

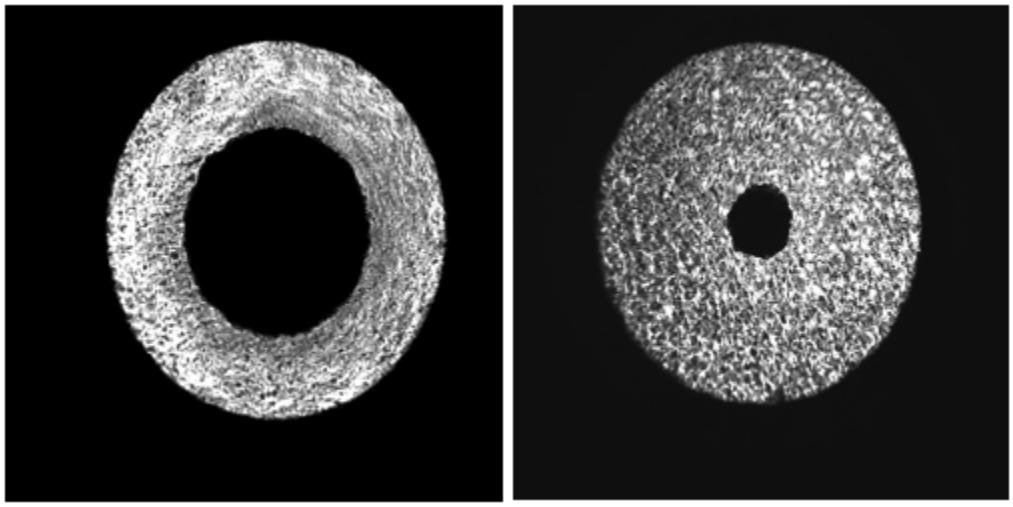

Fig. 9. CCD images of end faces for capillaries of 150 μm (left) and 50 μm ID using the apparatus in Fig 8.

readout power of the laser meter at the distal end and this value is recorded. Comparisons in light throughput for FOCaps of varying lengths for each ID can be made with this method (see results).

All fluorescence spectra obtained in later experiments (DTCC solutions and covalently attached pyrene) were acquired on a Fluorolog-3 (FL3-22, Jobin Yvon, F/# 3.6-3.8). The NA of the system (0.135) is smaller than that of the FOCap, so some emission light goes uncollected. When available, a laser light excitation source, which can be readily focused on a small area, is preferred and was used here to avoid illuminating the polyimide coating, which fluoresces upon excitation over a broad range in the visible spectrum (see section 3.3). As noted in the Introduction, removal of the polyimide coating to reduce this background fluorescence makes the exposed region (in

this case, just the end) very fragile. For our purposes in this set of experiments, where many separate capillaries were inserted and removed to and from apparatus over the course of the experiments, it was impractical to remove the polyimide coating. Moreover, the power and narrow bandwidth of a laser is better suited for EWFS.

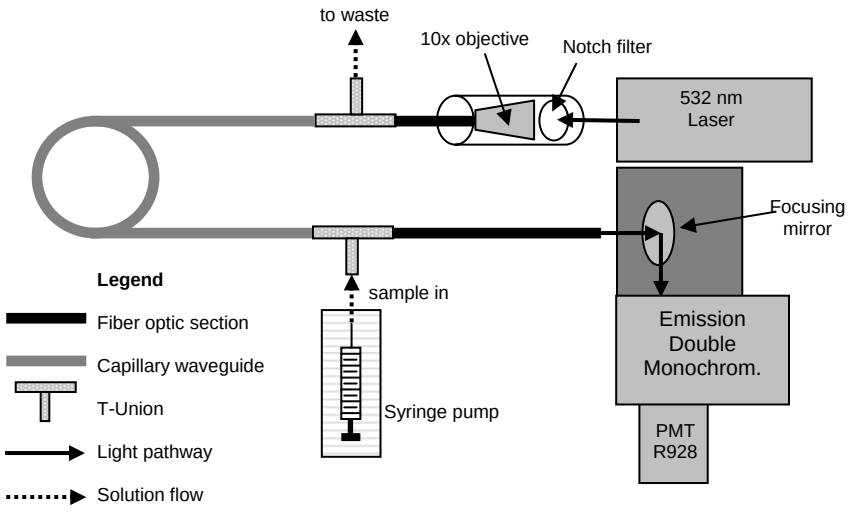

Fig. 10. Instrument diagram for capillary waveguide sensors for tests of bulk solutions. The light source is a 532 nm diode pumped solid state laser module. Light is coupled to the FOCap via a 10x microscope objective held in place by a machined part. Light is coupled into the Fluorolog system with a fiber optic coupler located in the sample chamber label the sample chamber via a focusing mirror (see blow up in Fig.11).

A schematic of the optical system used in testing the fluorescence guiding properties of FOCaps with a bulk fluorophore solution held in the core is shown in Fig. 10. In our coaxial approach, a laser diode module operating at 532 nm (GMP-532-3F3-CP, Lasermate) was used for excitation in the bulk solution case. The laser light passed through a notch filter (NT43-122, Edmund Optics), into a 10x objective (NT43-903, Edmund Optics) and illuminated the end face of a 400 μm optical fiber (FVP400440480, 0.22 NA, Polymicro Technologies, LLC). The distal end of the fiber was placed against

launch end of the sample FOCap in a custom built T-union. The other end of the FOCap was placed

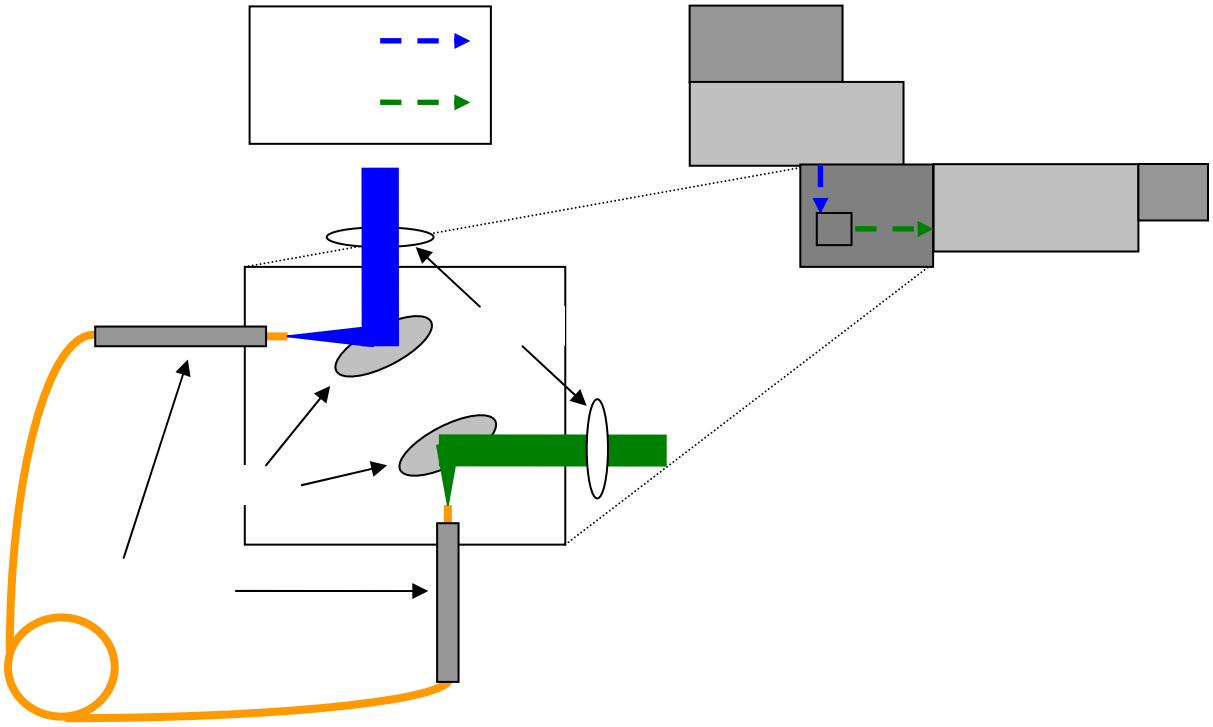

Fig. 11. Instrument diagram for capillary waveguide sensors with pyrene bound to the inner surface. The light source is a 450 W Xenon arc lamp. Light is coupled into the capillary and back into the Fluorolog system with a fiber optic coupler located in the sample chamber label the sample chamber via a focusing mirror.

against another 400 µm fiber optic in a T-union (Fig. 10). The T-unions allowed for injection of fluid while light is propagating through the FOCap. The end of the last fiber in the sequence was connected to the fluorescence system via a fiber optic coupler (Jobin Yvon, F-3000) held in the sample chamber of the Fluorolog-3. Excitation light was filtered out with a cut-on filter (550FG05-25, Andover Corp.), located just past the parabolic mirror of the coupler, and additionally with the Fluorolog-3 system's emission

double monochromator. The filtered emission was detected with a PMT (R928/0115/0381, Products for Research, Inc.) with a thermoelectric Peltier cooling system operating in photon counting mode.

When testing FOCaps covalently modified with pyrene (excitation 345 nm), the Fluorolog-3 system's 450-W Xe lamp and double monochromator proved sufficient and were used as the excitation source (Fig. 11). No laser source for this excitation wavelength range was readily available. For this set of experiments, excitation light was coupled directly into and out of the capillary (no fibers or T-Unions) via the fiber optic coupler. Prior to reaching the parabolic mirror of the coupler, light passes through a bandpass filter (HQ340/20X, Chroma). A cut on filter (365DCLP, Chroma) was again positioned just past the parabolic mirror on the emission side.

All optical components were covered to prevent exposure to ambient room light. Sufficient warm up time (~10 min.) was allowed for laser or lamp power to stabilize prior to making any measurements. Differences in excitation light intensity from sensor to sensor were accounted for by measurement of the light power at the distal end of the final 400 μm fiber or FOCap with the hand held laser power meter before and after each measurement. Emission intensities were normalized to the average of the excitation power.

3.2 Materials and Methods

FOCaps are available in three inner diameters (ID, n_0 in Fig. 5) of 50, 150, and 250 µm, each with an outer diameter of ~360 µm, and with a numerical aperture (NA) of 0.22 (LTSP series, Polymicro, LLC). The outer polyimide coating's thickness ranges from 18 to 20 µm. The doped layer is ? (~10 um from what I recall) – see brian's paper.???

To activate the inner surface, two 150 µm FOCaps were filled with 2 M NaOH solution. The solution was held in the capillaries for at least 2 h as Si-O-Si groups were converted to Si-OH groups, which are more reactive to certain silanes. This activation step was realized later in the project and was not performed when labeling the FOCaps with fluorescein. Aminopropyltrimethoxy silane (APTS, 0.5 M in water from 95% APTS, United Chemical Technologies, Inc.) was injected into the FOCap and placed

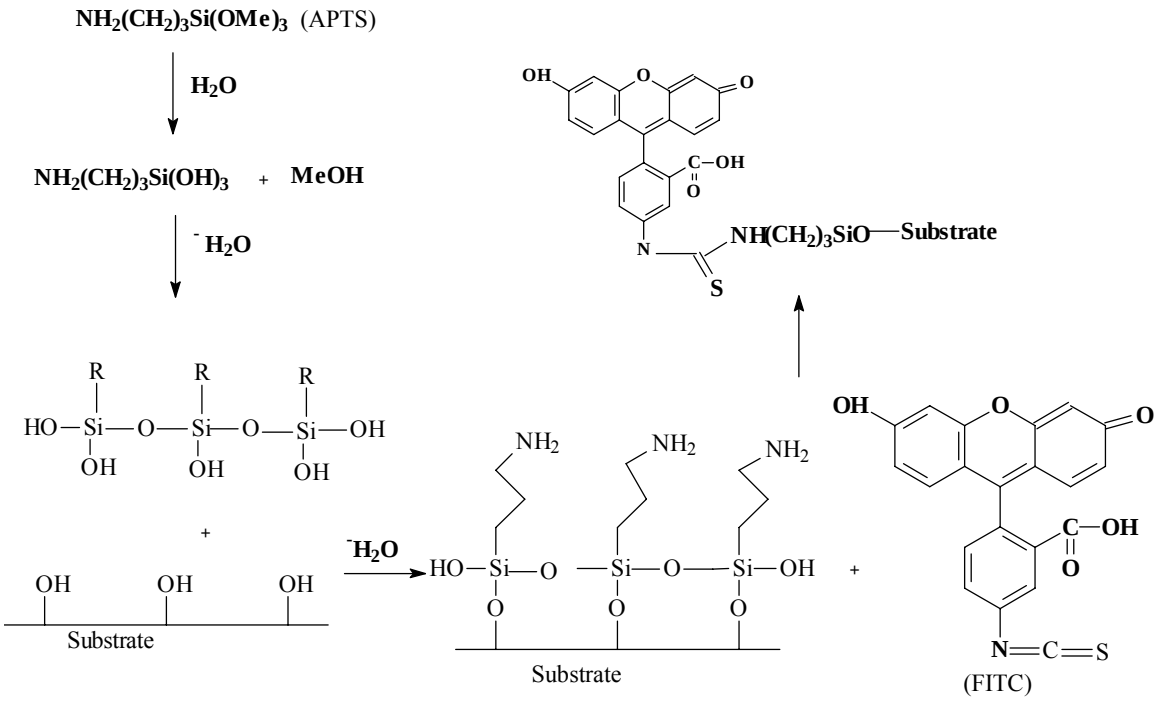

Fig. 12. Fluorescein labeling sequence.

in an 80°C water bath for 3-4 h after the ends of the capillary were sealed with a torch. The capillary was then opened and flushed with DI water and air. This was done after allowing the capillary to cool to room temperature for the fluorescein labeling and the pyrene labeling.

A $1x10^{-3}$ M solution of fluorescein-5-isothiocyanate (FITC 'Isomer I', F143, Molecular Probes) in DMF (EMD Chemicals Inc.) was prepared and injected into the modified capillary. The ends were sealed and the reaction was allowed to proceed overnight. The capillary was rinsed with DMF twice and then blown dry with air. Fig. 12 shows the entire labeling procedure for fluorescein.

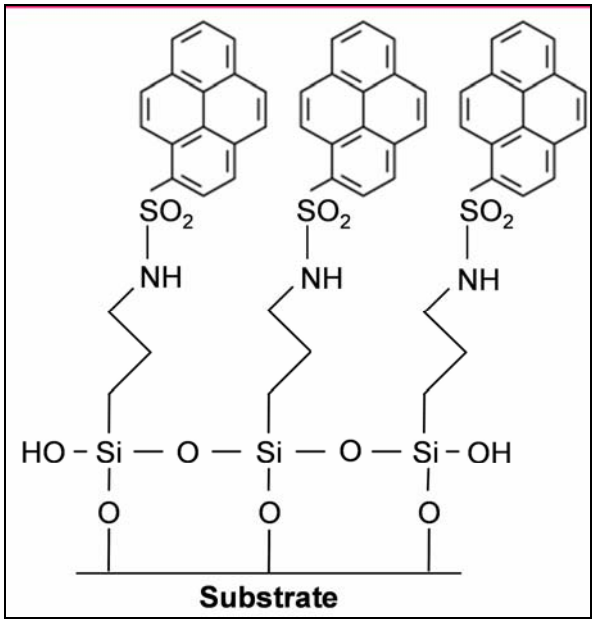

Fig. 13. Pyrene covalently attached to a FOCap.

As in the evanescent absorbance study of FOCaps[15], DTCC (Exciton, Inc.) was used to determine response dependence with capillary length, ID, and fluorophore

concentration for FOCaps with a bulk solution held in the core. Stock solution was made at 1.0 x 10^{-3} M in MeOH and diluted for the bulk fluorophore solution studies. The diluted solutions were manually loaded into the capillary through the T-Union by injection with a syringe. A background spectrum of only MeOH held in the core was acquired for each length tested of each ID. For each ID, a 20 m length of capillary was tested for sensitivity to four concentrations of DTCC. Capillary was cut to 15, 10, 4, 2 m lengths and again tested with each concentration. Capillary was rinsed between measurements with MeOH and the cut end faced was re-polished.

For the pyrene labeled experiments, a 1x10^{-3} M solution of 1-pyrenesulfonyl chloride (Molecular Probes) in DMF (EMD Chemicals Inc.) was prepared and injected into the modified (APTS) capillary after cooling to room temperature. The capillary was sealed and incubated in an ice/water bath (~4°C) overnight. The capillary was again rinsed and blown out with air. Test solutions were made from a stock solution of 2,4-DNT (1.0 x 10^{-2} M, Aldrich) in MeOH. Concentrations of solutions of 2,4-DNT ranged from 1.0 x 10^{-3} M to 1.0 M x 10^{-2} M. The probable final product of this labeling procedure is shown in Fig. 13.

3.3 Background fluorescence

In early experiments involving the excitation of FOCaps labeled with fluorescein, significant background fluorescence had to be overcome. In latter experiments, the strength (lower relative to signal) and features of background spectra were more reproducible. Labeling techniques and light coupling techniques had improved to where a simple subtraction of the background fluorescence spectrum for a given length and ID for a FOCap was appropriate. Relative intensities of background fluorescence for varying excitations of a bare FOCap are shown in Fig. 14. Polyimide fluoresces more when excited at shorter wavelengths. For fluorescein-labeled FOCaps, the large background signal (~35% of total fluorescence) was almost completely eliminated by removal of the polyimide coating 0.5 cm back from the end faces, however this made handling FOCaps difficult due to the brittleness of the exposed ends. As such, for DTCC and pyrene experiments, this technique was less ideal given the volume of sample capillaries being exchanged. The improved relative intensity of the background fluorescence versus FOCap plus fluorophore fluorescence (~7 to 10%) also permitted this procedure to be used. The background subtracted from each sensor sample was representative of the optical fibers and capillaries used in making the sample measurement and was reproducible. For example, in a DTCC experiment (Fig. 10) the background spectrum was from the same setup to be used in making the DTCC measurement without the DTCC, including all fibers, T-unions, filters, and the solvent.

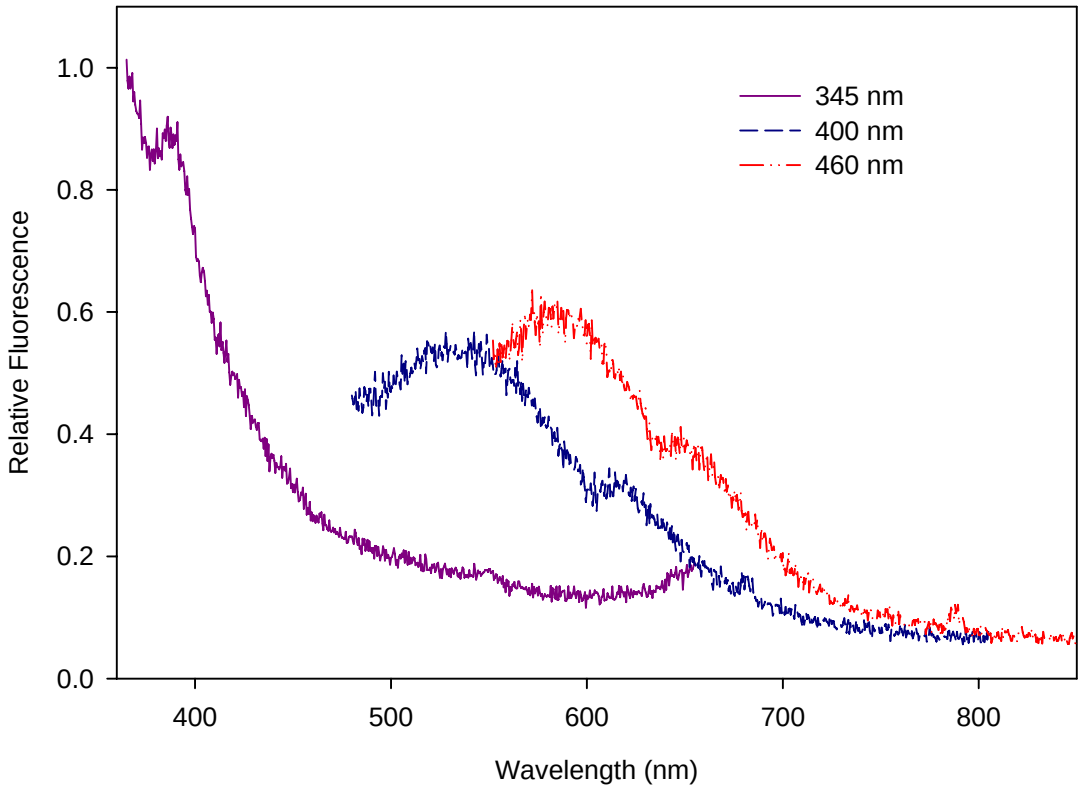

Fig. 14. FOCap background fluorescence. Spectra acquired for an unmodified, air filled, 10 m 150 µm capillary with the Fluorolog (5 nm bandpass) and normalized to constant excitation intensity as measured by the power meter at the distal end.

For DTCC measurements, this background subtraction was made in addition to the interfacial fluorescence subtraction, described in section 3.4. The background signal was not length dependent. No attempt was made to control the temperature at which spectra were acquired (room temperature).

3.4 Interfacial fluorescence

For DTCC measurements, fluorescence from the interfacial regions where the capillary end faces were butted against the fiber end faces was subtracted from the overall fluorescence spectrum. The magnitude of this interfacial fluorescence is dependent on capillary ID, concentration of the dye, and the excitation light intensity. Background-corrected fluorescence plotted against capillary length for each ID at each concentration tested fit the equation:

$$F_{tot} = b_{cap} \times F_{ev} + F_{i,} \qquad (8)$$

where the total fluorescence (F_{tot}) is a function of the pathlength times the evanescent fluorescence (F_{ev}) and the interfacial fluorescence (F_i) for any capillary length for a given concentration of DTCC and for a particular ID is the y-intercept of each least squares fit[15]. Interfacial fluorescence was never over ~7% of total fluorescence, and was significantly lower than that for longer length, 250 μm ID FOCaps. The thinner end faces of the larger ID FOCaps illuminate less area than thicker walled FOCaps.

Chapter 4.

Results and Discussion

4.1 Light throughput of FOCaps

The reported (Fig. 2) nearly lossless optical transmission properties of FOCaps were confirmed. Tests varying ID (wall thickness), length of capillary, and wavelength of light show very little variability from sample to sample (Table 1). Only capillary IDs of 150 μm and 50 μm were tested. The 250 μm ID FOCap's wall thickness proved too brittle to polish (at the time) effectively and thus light coupling was not reproducible. Roughly 40% transmission (light out of pinhole versus light out of distal capillary end) is reported for all. This value is largely controlled by losses from scattering and reflection when coupling light at the proximal and distal ends of the FOCap. The nearly constant value also confirms that the mechanical end face polishing is effective and reproducible.

Table 1. Percent light throughput as a function of capillary ID, length, and wavelength.

	Capillary length (λ = 460 nm)			Wavelength (50 μm ID, 1 m in length)		
ID	0.50 m	2.0 m	3.0 m	400 nm	460 nm	545 nm
50 μm	37 (1.2)*	39 (0.7)	41 (0.8)	41 (1.2)	42 (0.7)	43 (4.5)
150 μm	39 (0.9)	39 (0.3)	39 (0.8)	n.d.	n.d.	n.d.

*Values reported as a percentage. Numbers in parentheses are standard deviations for n =10. n.d.= not determined

4.2 Evanescent fluorescence from a fluorescein labeled FOCap

Over the lengths and measurements examined, a uniform labeling procedure was assumed with fluorescein isothiocyanate (FITC) in FOCaps. Spectra for 1 to 4 m lengths of 150 μm FOCaps are shown in Fig. 15. A plot of peak fluorescence at 524 nm against capillary length indicates a linear trend with an R^2 value of 0.9937 (Fig. 16). A lack of overall signal and high noise indicated poor labeling. In later labeling work with pyrene, a surface activation with NaOH was performed, which increased the amount of Si-OH groups available for attachment of APTS.

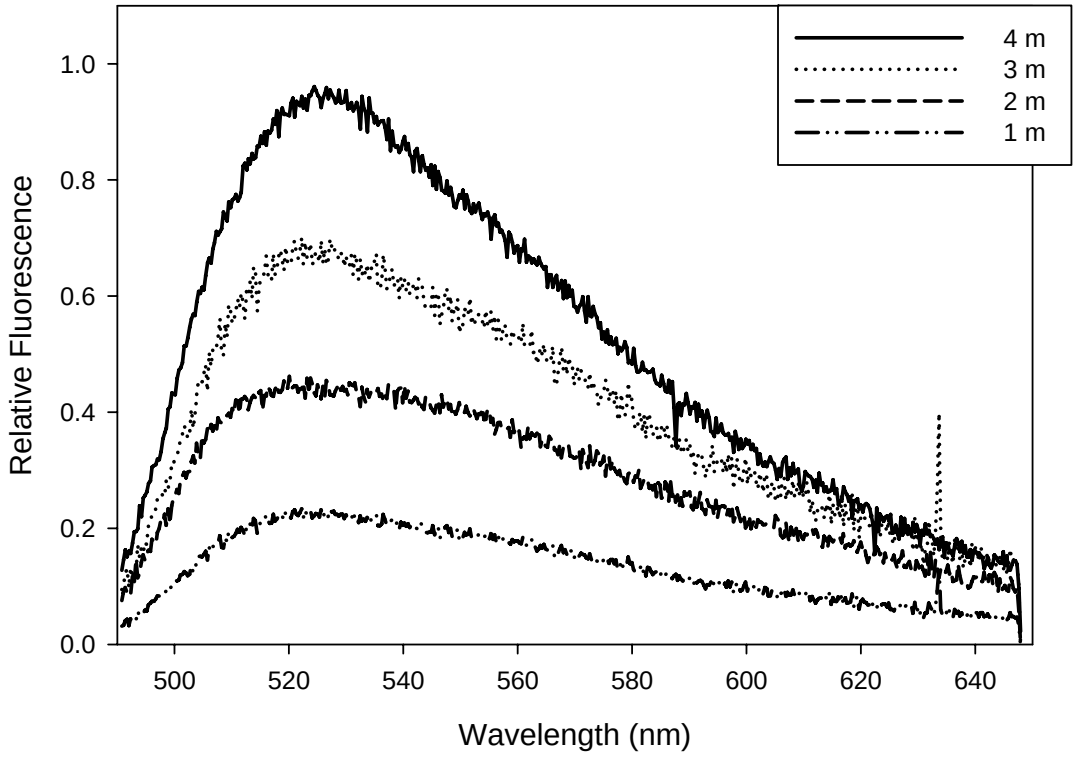

Fig 15. Background-corrected fluorescence spectra for different length fluorescein labeled FOCaps (150 μm, air dried) normalized for light intensity.

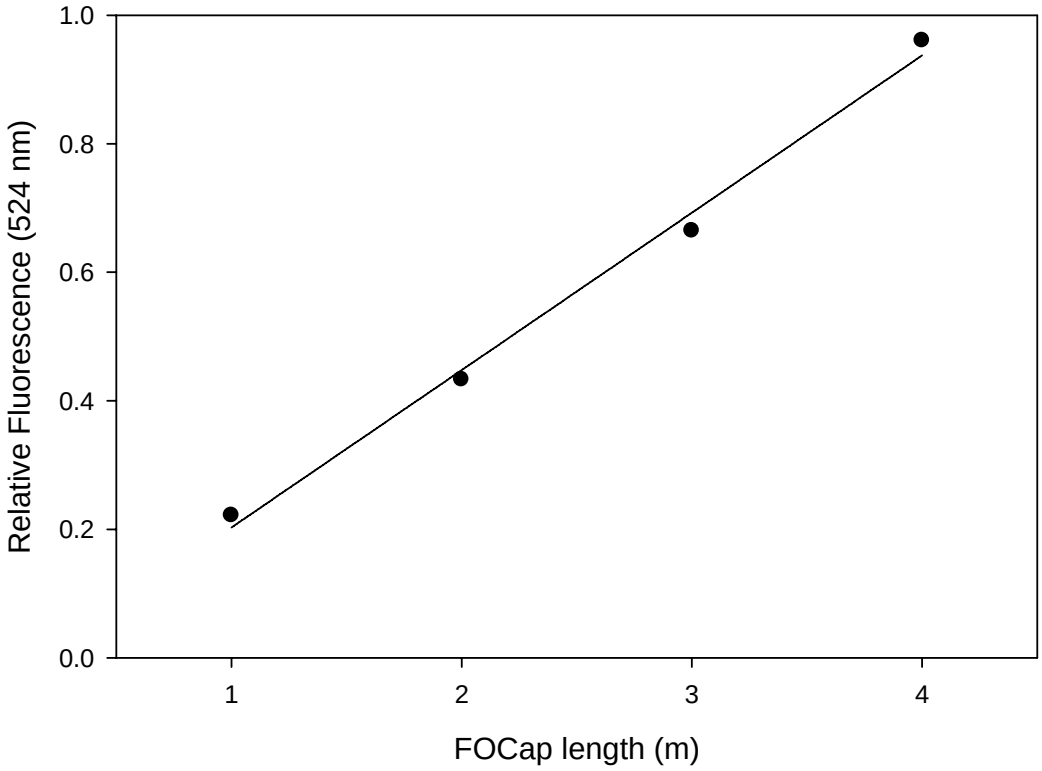

Fig 16. FOCap length against relative peak fluorescence for 150 μm fluorescein labeled FOCaps ($R^2 = 0.9937$).

4.3 Evanescent fluorescence from solutions in FOCaps

Peak normalized fluorescence spectra for DTCC (0.001 M) in a cuvette and in a 4 m 150 μm FOCap are shown in Fig. 17. The shoulders of the evanescent DTCC spectrum appear more pronounced and the peak emission is shifted slightly. Peak emission is shifted to a longer wavelength for DTCC solution held in the FOCap due to the wavelength dependence of depth of penetration (Equation 3). Longer wavelengths more effectively penetrate and hence enhance emissions at longer wavelengths. Stimulated fluorescence is proportional to the local electric field intensity.

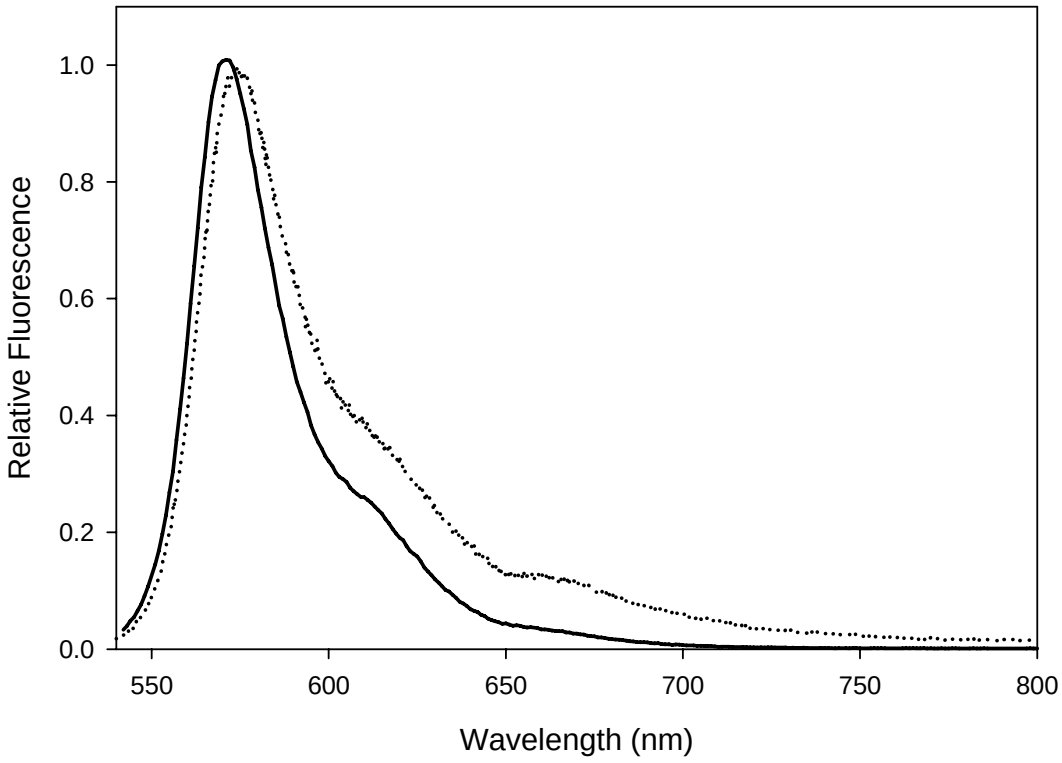

Fig. 17. Peak normalized fluorescence spectra of DTCC in a cuvette (solid line) and in a 4m 150 μm ID FOCap (dotted line).

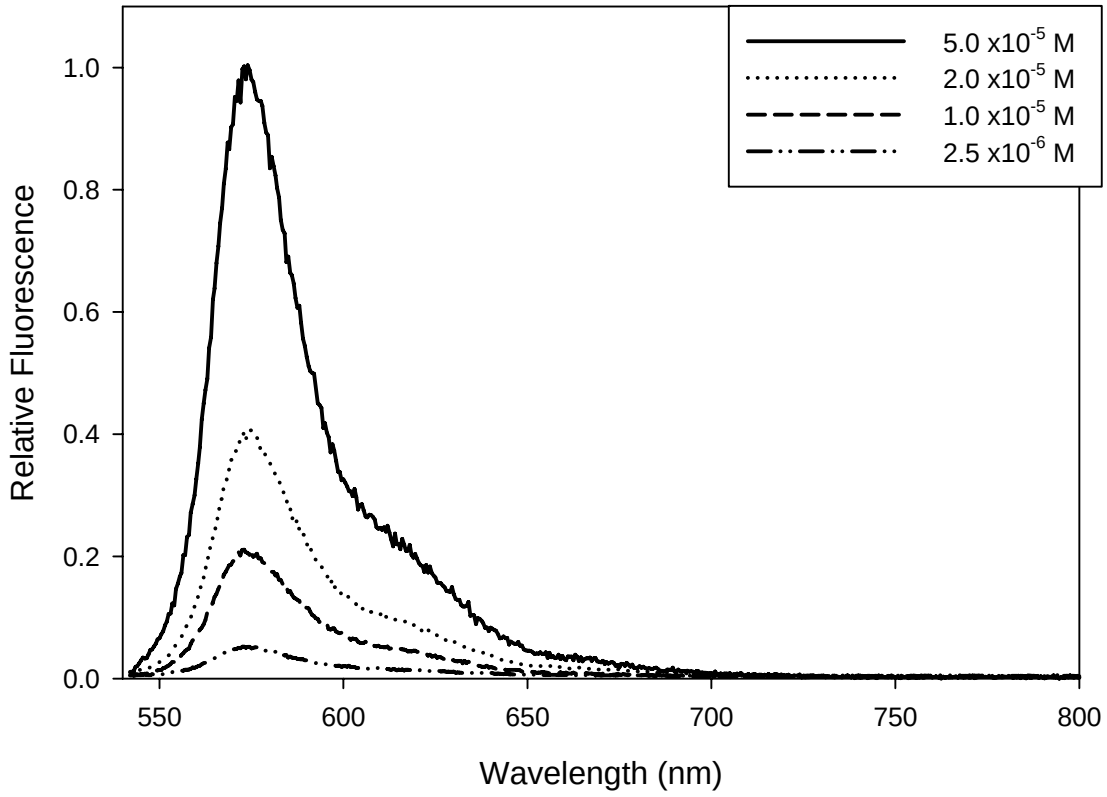

Fig. 18. Spectra of DTCC in MeOH at concentrations of 5 x 10^{-5}, 2.0 x 10^{-5}, 1.0 x 10^{-5}, and 2.5 x 10^{-6} to M DTCC in MeOH from a 2 m long, 150 μm ID FOCap with MeOH blank. Spectra contain contributions from evanescent fluorescence detection in the waveguide and the interfacial regions.

Fluorescence spectra for 2.5 x 10^{-6} to 5 x 10^{-5} M DTCC in MeOH from a 2 m long 150 μm ID FOCap are shown in Fig. 18. There is a contribution to the total fluorescence from the interfacial regions between the fiber and capillary faces in the T-unions, as seen in the evanescent absorbance FOCap study [17].

4.4 FOCap evanescent fluorescence versus capillary length and ID

The evanescent fluorescence relationship with capillary length was found to be nearly linear (R^2 in the range of 0.980 to 0.995) up to the longest length tested (20 m) as seen in Fig. 19 for a 250 μm ID FOCap and as predicted by theory for low concentrations within the evanescent absorbance linear range (Equation 6). The non-linear appearance in these measurements can possibly be attributed to the way measurements were made. Each DTCC concentration was run for each length, then the capillary was cut and the concentration range was rerun for the next, shorter length. Therefore, for example, the 20 m values could all be systematically low and 15 m systematically high due to an error in

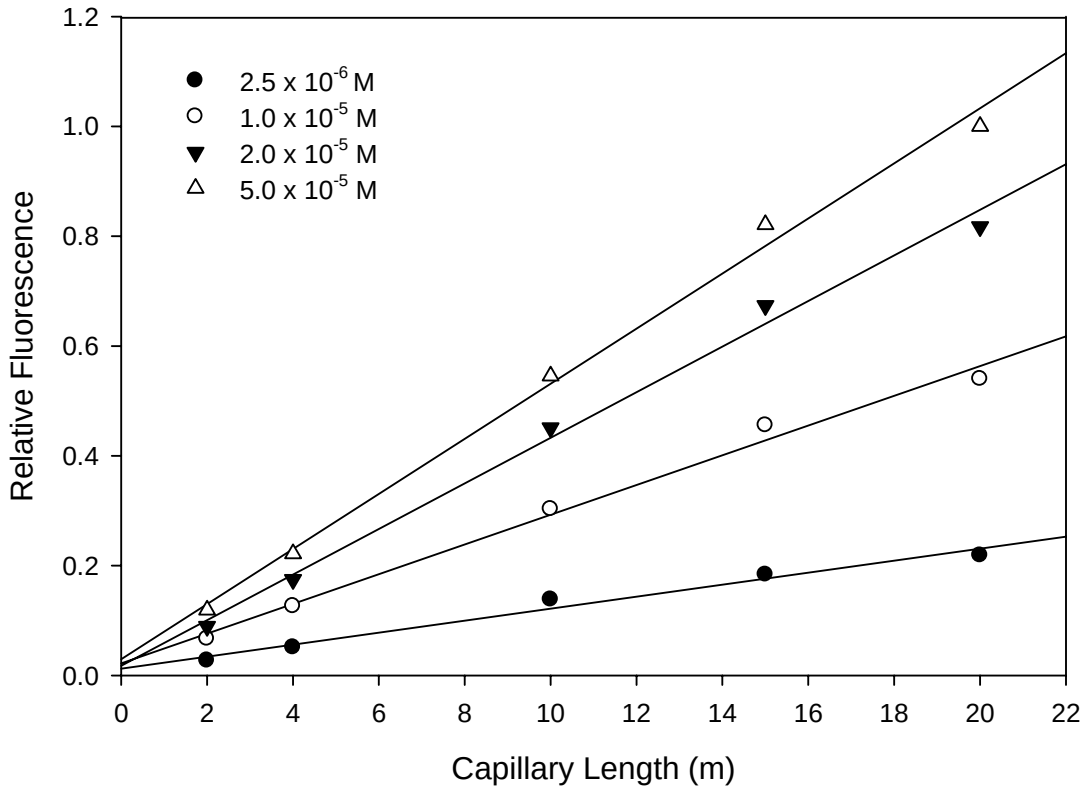

Fig. 19. Evanescent fluorescence for varying concentrations of DTCC in MeOH in 250 μm ID FOCap is nearly linear to 20 m. Data are corrected for interfacial fluorescence.

measurement carried from length to length. One possible explanation for this could be a larger than normal interfacial gap at the proximal end of the fiber producing an interfacial fluorescence greater than that subtracted out. Data from 150 μm and 50 μm ID FOCaps do not show the same non-linearity (Fig. 20 and Fig. 21).

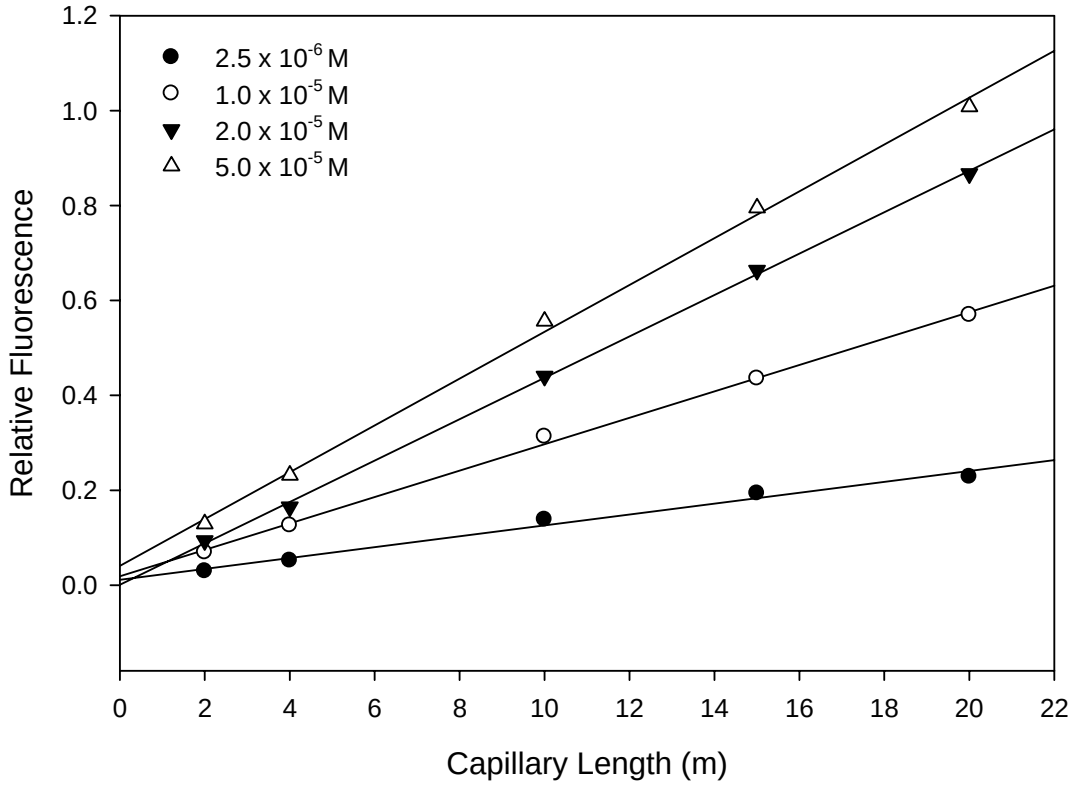

Fig. 20. Evanescent fluorescence for varying concentrations of DTCC in MeOH in 50 μm ID FOCap is linear to 20 m. Data are corrected for interfacial fluorescence.

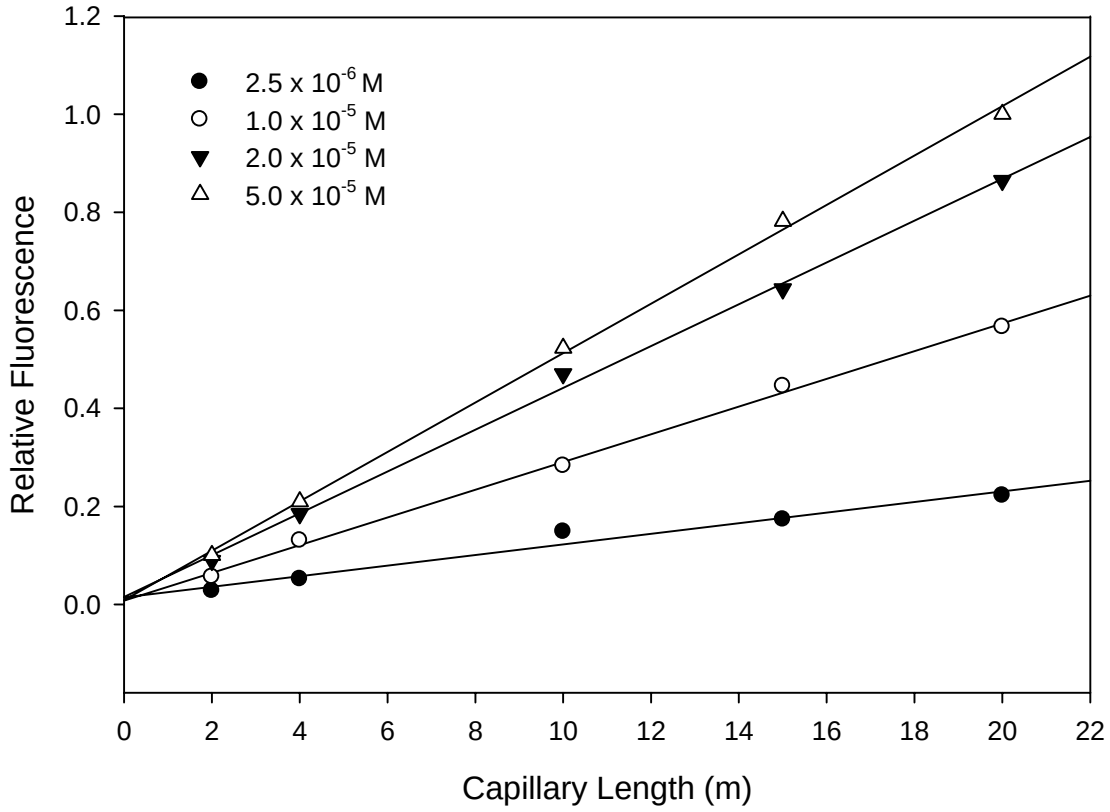

Fig. 21. Evanescent fluorescence for varying concentrations of DTCC in MeOH in 150 μm ID FOCap is linear to 20 m. Data are corrected for interfacial fluorescence.

Evanescent fluorescence dependence on FOCap ID was also tested (Fig. 22). Thinner-walled capillaries have more internal reflections than thick-walled capillaries and thus have a higher sensitivity. A plot of $1/\rho$ versus relative fluorescence for the data in Fig. 22 shows an increase in fluorescence sensitivity with inverse wall thickness (Fig. 23).

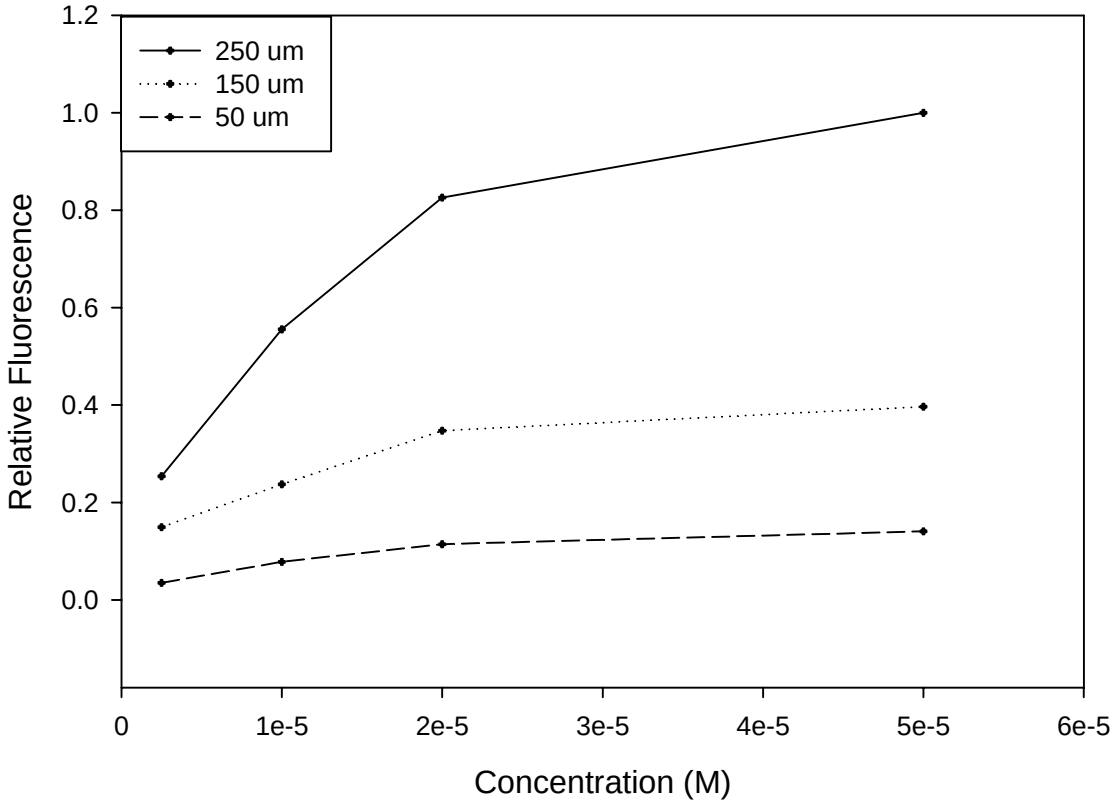

Fig. 22. Evanescent fluorescence of DTCC in MeOH in capillaries of 3 different IDs all 10 m in length. Thinner-walled capillaries have more sensitivity.

We compare the sensitivities of the different FOCap configurations by calculating the number of reflections in each configuration assuming a propagation angle of 8.6° [15]. The relative reflection ratio is then calculated by normalizing to the number of reflections in the 50 um ID waveguide. Any angle gives the same theoretical reflection ratio as this

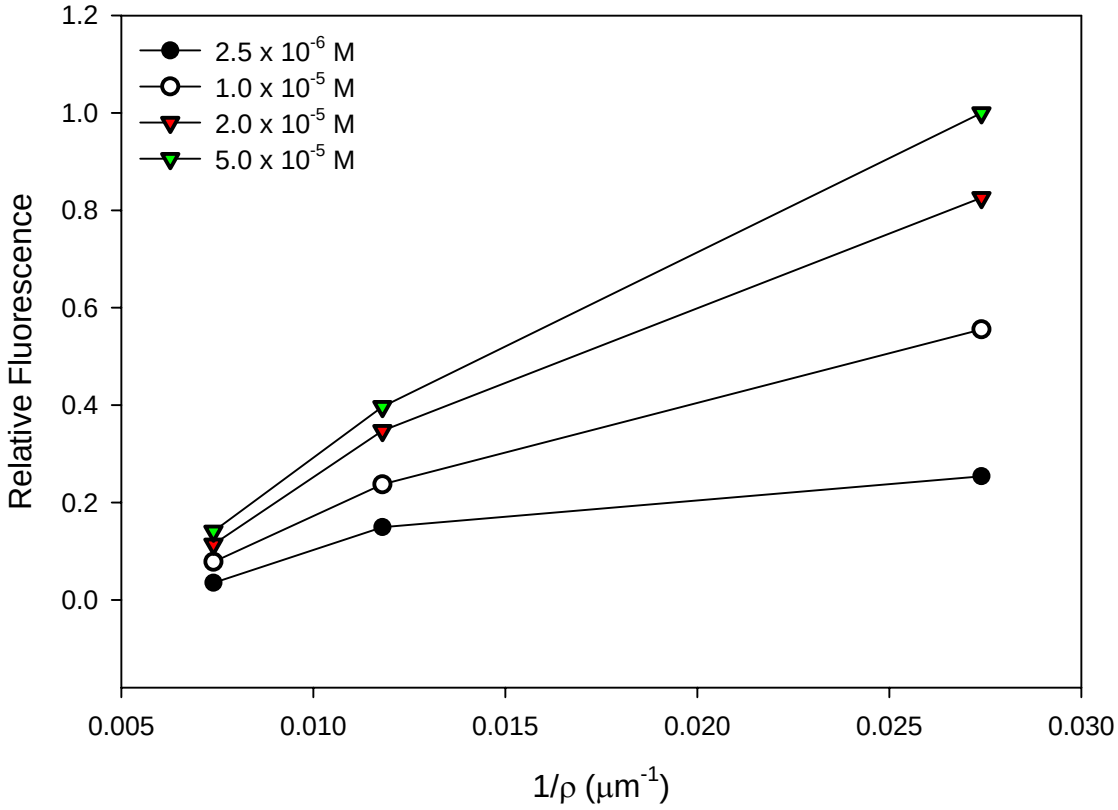

Fig. 23. Relative fluorescence versus inverse wall thickness for each concentration tested (Fig. 22).

parameter is a measure of the relative sensitivity between the various ID FOCaps. For the data presented in Fig. 22, the evanescent fluorescence values for the 150 and 250 μm ID measurements were divided by the 50 μm ID measurements to find the experimentally determined sensitivity ratios. Table 2 lists the reflections per meter, experimental sensitivity ratios from absorbance and fluorescence measurements, and calculated

Table 2
Theoretical reflection ratios and experimental FOCap sensitivity ratios calculated from the FOCap evanescent fluorescence data presented in Fig. 5.

FOCap ID (μm)	Reflections/m (θ =8.6°)	Experimental Sensitivity Ratio (Abs., Keller, *et al*.)	Experimental Sensitivity Ratio (Fluor.)	Theoretical Sensitivity Ratio
50	650	1 (normalized)	1 (normalized)	1 (normalized)
150	1130	2.0 ± 0.9	1.5± 0.8	1.7
250	4480	6.5 ± 1.2	7.2 ± 0.9	6.9

reflection (sensitivity) ratios. The sensitivity ratios calculated from the fluorescence data match reasonably well with calculated ratios and the ratios determined from the absorbance study.

Table 3 lists the experimentally determined limits of detection (LOD) for DTCC for the different FOCaps lengths and IDs. Generally, thinner walled and longer capillaries have the lowest LODs due to more EW generating reflections. The estimated LOD for DTCC in MeOH in a cuvette with our fluorometer was 1.21×10^{-9} M; consequently, the FOCap is ~1-2 orders of magnitude less sensitive than conventional fluorescence spectrophotometry at this excitation wavelength.

Table 3
Limit of detection (M) for DTCC for each length for each ID.

FOCap length	50 μm	150 μm	250 μm
2 m	2.8×10^{-7}	2.3×10^{-7}	1.8×10^{-7}
4 m	9.0×10^{-8}	9.8×10^{-8}	6.2×10^{-8}
10 m	6.9×10^{-8}	7.1×10^{-8}	5.9×10^{-8}
15 m	6.5×10^{-8}	7.2×10^{-8}	5.1×10^{-8}
20 m	5.2×10^{-8}	5.6×10^{-8}	3.0×10^{-8}

4.5 FOCap 2,4-DNT sensor based on quenching of pyrene fluorescence

As described above, An EW fluorosensor was constructed with FOCaps for indirect detection of 2,4-DNT and to determine evanescent sensitivity with length of capillary for the covalently bound fluorophore case. Pyrene fluorescence dependence on length of capillary is shown in Fig. 24 for a 150 μm capillary. A 15 m length of FOCap was labeled, tested and then cut for the next measurement.

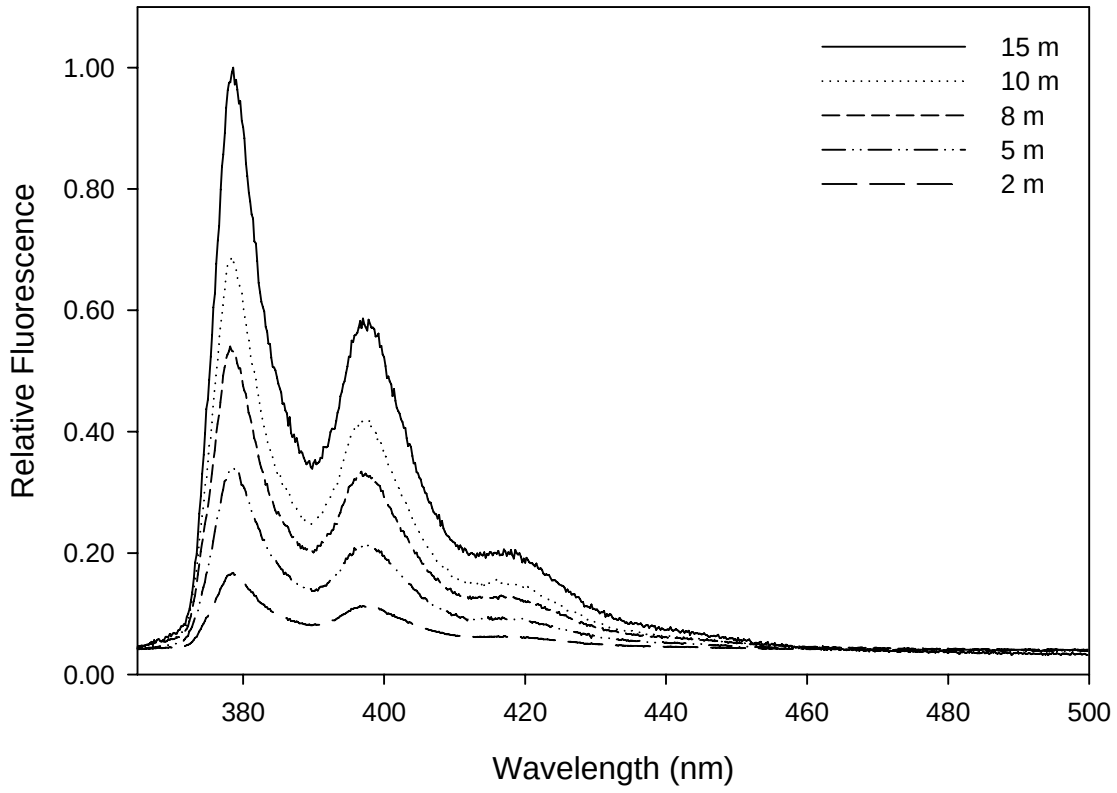

Fig. 24. Evanescent fluorescence spectra of immobilized pyrene in different length 150 μm ID capillaries.

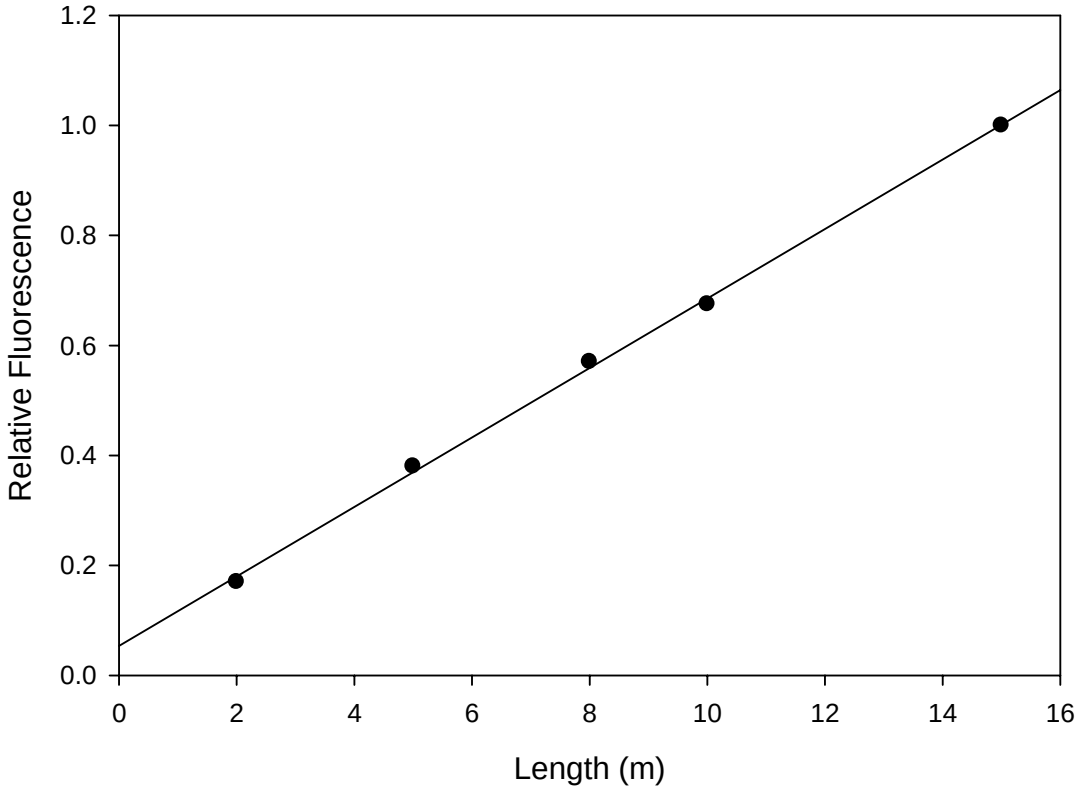

Fig. 25. Peak evanescent fluorescence of immobilized pyrene (Fig. 24) in different length 150 μm ID capillaries.

A plot of peak fluorescence versus length yields an R^2 value of 0.98 (Fig. 25). Based on the linear trend with length, a uniform labeling along the capillary length was achieved.

To test the utility of a pyrene labeled FOCap as an indirect sensor for 2,4-DNT, two 10 m lengths were also labeled with pyrene with the procedure previously outlined, and tested for sensitivity to 2,4-DNT. The Stern-Volmer plot in Fig. 26 shows a linear response in the concentration range tested for the two trials. Some decline in overall

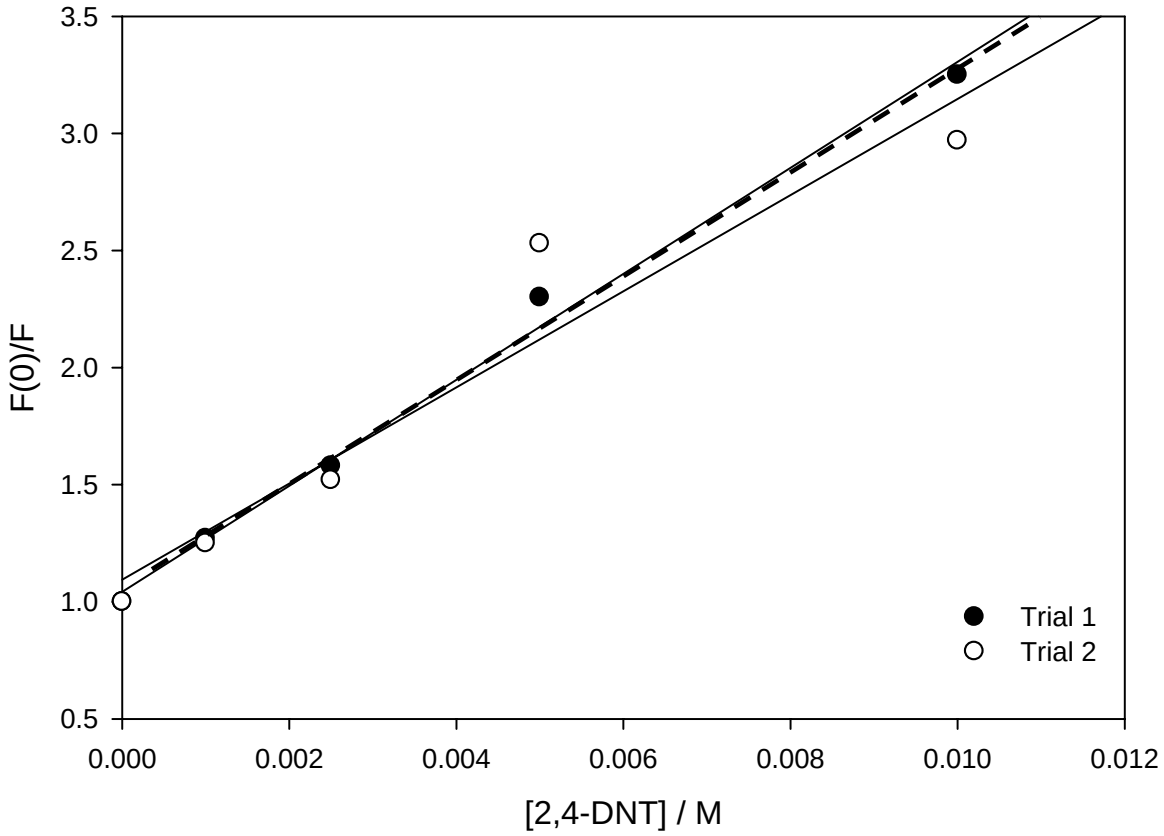

Fig. 26. Stern-Volmer plot for 2,4-DNT quenching of pyrene by a dynamic mechanism. 10 m, 150 um ID FOCaps were labeled with pyrene and tested with concentrations of 2,4-DNT in MeOH. The Stern-Volmer constants were 226 M^{-1} (black dots, dashed line) and 205 M^{-1} for trials 1 ($R^2 = 0.98$) and 2 ($R^2 = 0.92$), respectively.

signal was observed over time and with each use possibly due to loss of adsorbed dye and some loss of dye covalently linked to the capillary wall. However, F_0/F response with quencher concentration did not change with loss of overall signal. To acquire pyrene spectra, capillaries had to be filled, then manually inserted into place in the experimental apparatus, so the response time could not be determined. Because there is no membrane to create a diffusional barrier, theory suggests response time is on the order of the excited

state lifetime of the fluorophore. The mean LOD for the two trials was 0.0008 M 2,4-DNT in MeOH. The LOD is limited by the low light throughput in the coaxial experimental setup utilizing the lamp from the fluorometer as the light source. Stern-Volmer constants (the slopes in linear regressions) for the two trials were similar (226 M^{-1} and 205 M^{-1}). A value of 386 for pyrene quenching by 2,4-DNT in acetonitrile has been reported in the literature[19], however comparing to our results would not be appropriate as the fluorescence life time (τ_0) would not be comparable.

FOCaps show enhanced sensitivity compared to a previous short length capillary waveguide sensor with LODs improved by 1-2 orders of magnitude and FOCaps show a similar reproducibility (F_0/F) to other waveguide fluorescence quenching sensors[9].

Chapter 5
Conclusions and Future Work

Commercially available FOCaps were tested for fluorescence sensitivity to fluorophore solutions held in the core and to fluorophores covalently bonded to the capillary wall utilizing various instrument schemes. FOCap light throughput was nearly lossless over long lengths, various IDs, and various wavelengths. Emission spectra for the fluorophores studied are pushed to longer wavelengths due to the wavelength dependence of the depth of penetration. Thin-walled (250 μm) capillaries were found to have much greater fluorescence sensitivity (~7x) than thick-walled capillaries (50 μm) when a DTCC solution is held in the core. The optical sensing of the FOCap is linear to long lengths of capillary for low concentration solutions of fluorophore, indicating a homogenous transducer surface along the capillary bore hole.

Homogeneous labeling procedures were established for fluorescein and pyrene binding along the length of the FOCap inner surface. Enhanced binding of pyrene in later experiments was achieved by using a surface activation prior to reaction with APTS, the linker compound. This surface activation converted more of the Si-O-Si groups to Si-OH groups. Evanescent fluorescence was found to be linear with length to 4 m and 15 m with covalently attached fluorescein and pyrene, respectively.

An indirect chemical sensor based on the pyrene-labeled FOCap was constructed for a common explosive breakdown/byproduct. 2,4-DNT effectively and reproducibly quenched pyrene fluorescence, as indicated by similar Stern-Volmer constants.

Separate optical testing systems were devised for each fluorophore examined. Sufficient filtering and additional excitation light rejection with a double monochromator allowed a coaxial approach to be used for pyrene and DTCC. Procedures were established for subtraction or removal of background fluorescence from the polyimide coating. Removal of the coating from the end faces (where light is coupled into the FOCap) eliminated this source of background and should be done whenever practical. Interfacial fluorescence from fluorophore solution held between fiber and capillary was accounted for and should be subtracted from measurements when using T-unions or similar opto-fluidic connectors.

FOCap LOD's hold an important advantage over other capillary waveguides with their ability to be fined tuned (length and ID) for a particular application/need. The ability to flush samples through the FOCap does become an increased concern when considering very long lengths. Need for removal of polyimide coatings from optical points of entry and exit should also always be considered when using FOCaps.

Enhancement in sensitivities of FOCaps could be made through further fine tuning of the optical system and pumping systems. Collecting emission light in the opposite direction of the propagation of excitation light would improve signal to noise by eliminating the need for some of the optical filtering. The removal of the double monochromator would greatly improve signal. A better sample pumping system would allow the use of longer length capillaries and improve sensitivity. To achieve a better sample pumping, improvements to alignment tolerances of fibers and capillaries would be needed.

References

(1) Taitt, C. R. A., George P. ;Ligler, Frances S. *Biosensors and Bioelectronics* **2005**, *20*, 2470-2487.
(2) Brandenburg, A.; Edelhaeuser, R.; Werner, T.; He, H.; Wolfbeis, O. S. *Mikrochimica Acta* **1995**, *121*, 95-105.
(3) Yamakawa, S. *Sensors and Materials* **1997**, *9*, 187-196.
(4) Ahmad, M.; Chang, K.-P.; King, T. A.; Hench, L. L. *Sensors and Actuators, A: Physical* **2005**, *A119*, 84-89.
(5) Wolfbeis, O. S. *Anal Chem* **2006**, *78*, 3859-74.
(6) Culshaw, B. D., J. *Optical Fiber Sensors*; Artech House, 1996.
(7) DeGrandpre, M. D., and Burgess, L.W. *Anal. Chem.* **1988**, *60*, 2582.
(8) Weigl, B. H.; Wolfbeis, O. S. *Analytical Chemistry* **1994**, *66*, 3323-7.
(9) Wolfbeis, O. S. *TrAC, Trends in Analytical Chemistry* **1996**, *15*, 225-232.
(10) Dhadwal, H. S.; Kemp, P.; Aller, J.; Dantzler, M. M. *Analytica Chimica Acta* **2004**, *501*, 205-217.
(11) Ertekin, K.; Klimant, I.; Neurauter, G.; Wolfbeis, O. S. *Talanta* **2003**, *59*, 261-267.
(12) Hart, S. J. *Proceedings of SPIE-The International Society for Optical Engineering* **2001**, *4201*, 112-117.
(13) Weigl, B. H.; Wolfbeis, O. S. *Proceedings of SPIE-The International Society for Optical Engineering* **1994**, *2293*, 54-63.
(14) Kessler, M. A.; Hubmann, B. A.; Dremel; Wolfbeiss *Clinical Chemistry* **1992**, *38*, 2089.
(15) Keller, B. K.; DeGrandpre, M. D.; Palmer, C. P. *Proceedings of SPIE-The International Society for Optical Engineering* **2004**, *5585*, 143-151.
(16) Tao, S.; Gong, S.; Fanguy, J. C.; Hu, X. *Sensors and Actuators, B: Chemical* **2007**, *B120*, 724-731.
(17) Keller, B. K.; DeGrandpre, M. D.; Palmer, C. P. *Sensors and Actuators B: Chemical*, *In Press, Corrected Proof*.
(18) Lippitsch, M. E.; Draxler, S.; Kieslinger, D.; Lehmann, H.; Weigl, B. H. *Applied Optics* **1996**, *35*, 3426-3431.
(19) Goodpaster, J. V.; McGuffin, V. L. *Analytical Chemistry* **2001**, *73*, 2004-2011.
(20) Fetterolf, D. D. *Forensic Appl. Mass Spectrom.* **1995**, 45-57.
(21) Nambayah, M.; Quickenden, T. I. *Talanta* **2004**, *63*, 461-467.
(22) Toal, S. J.; Trogler, W. C. *Journal of Materials Chemistry* **2006**, *16*, 2871-2883.
(23) Oxley, J. C. *Proceedings of SPIE-The International Society for Optical Engineering* **1995**, *2511*, 217-26.
(24) Snyder, A. W., and Love, J.D. *Optical Waveguide Theory*; Chapman and Hall: New York, 1983.
(25) Glass, T. L., Steve; Hirschfeld, Tomas *Applied Optics* **1987**, *26*, 2181-2187.
(26) Carniglia, C. K.; Mandel, L.; Drexhage, K. H. *Journal of the Optical Society of America* **1972**, *62*, 479-486.
(27) Lakowicz, J. R. *Principles of Fluorescence Spectroscopy*; Plenum Press: New York, 1983.
(28) Guilbault, G. *Practical Fluorescence*; Marcel Dekker, Inc.: New York, NY, 1973.

(29) Kao, H. P.; Schoeniger, J. S. *Applied Optics* **1997**, *36*, 8199-8205.
(30) Kieslinger, D.; Weigl, B. H.; Draxler, S.; Lippitsch, M. E. *Optical Review* **1997**, *4*, 85-88.